ON THE SPECTRUM AND POLARIZATION OF MAGNETAR FLARE EMISSION

Roberto Taverna – Roberto Turolla
Department of Physics and Astronomy
University of Padova

Outline

- ❑ Introduction - Magnetars
- ❑ Theoretical model
- ❑ Numerical implementation
- ❑ Conclusions and Future prospects

Introduction - Magnetars

Magnetars - Basics

- Magnetars are isolated Neutron Stars powered by their own magnetic energy, observationally identified with SGRs and AXPs
  - $L_X \sim 10^{33} - 10^{36}$ erg/s $> \dot{E}$
  - $B \gtrsim B_{\rm QED}$ (at least inside the star)

$$B = 3.2 \times 10^{19} \sqrt{P\dot{P}}\ \mathrm{G}$$

$$B \sim 10^{14}\ \mathrm{G}$$

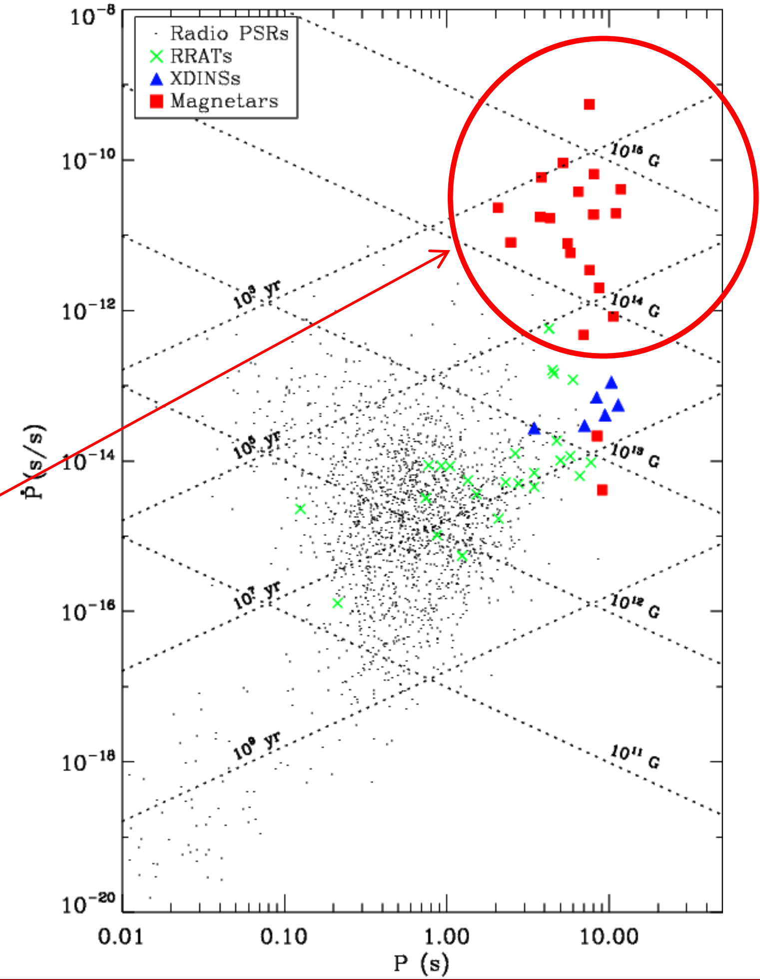

Magnetars - Basics

- Magnetars are isolated Neutron Stars powered by their own magnetic energy, observationally identified with SGRs and AXPs
  - $L_{\mathrm{X}} \sim 10^{33} - 10^{36}\ \mathrm{erg/s} > \dot{E}$
  - $B \gtrsim B_{\mathrm{QED}}$ (at least inside the star)

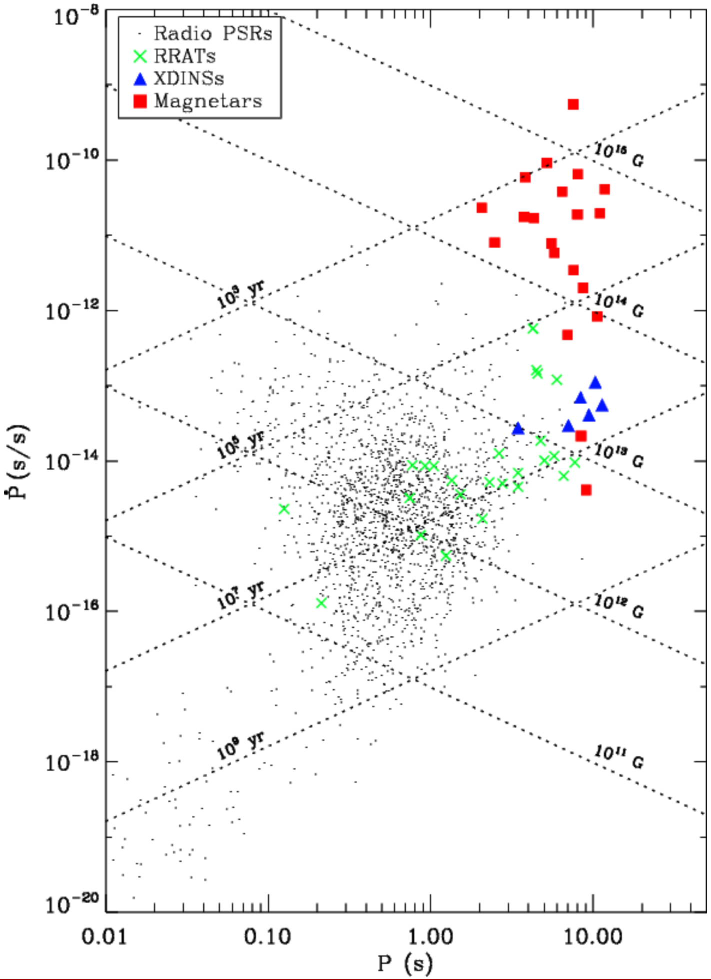

- Persistent emission
  - Soft X-ray spectrum $(0.5\ - 10\ \mathrm{keV})$ BB + PL (or BB + BB)
  - Additional PL for $E \gtrsim 20\ \mathrm{keV}$

Magnetars - Basics

- Bursting activity
  - Giant flares

$$\Delta t_{\text{spike}} \sim 0.1 - 1 \text{ s}$$
$$\Delta t_{\text{tail}} \sim 10^2 - 10^3 \text{ s}$$
$$E = 10^{44} - 10^{47} \text{ erg}$$

  - Intermediate flares

$$\Delta t \sim 1 - 10^2 \text{ s}$$
$$E \sim 10^{41} - 10^{43} \text{ erg}$$

  - Short bursts

$$\Delta t \sim 0.01 - 1 \text{ s}$$
$$E \sim 10^{36} - 10^{41} \text{ erg}$$

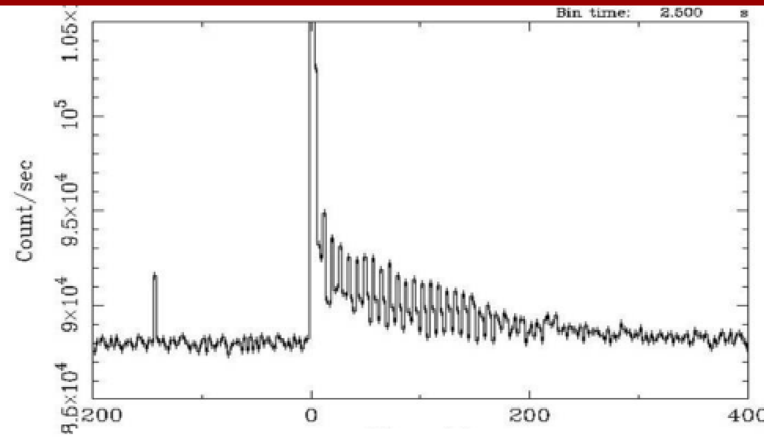

Mereghetti S. 2008, A&A, REV 15, 225

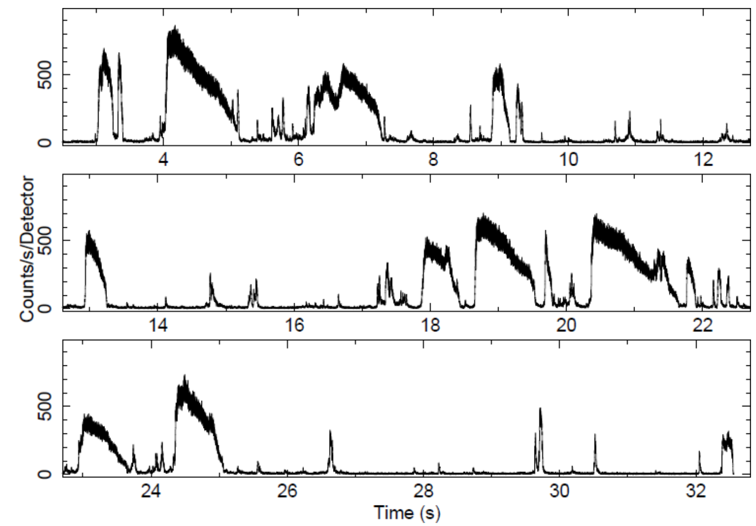

Israel et al., 2008, ApJ, 685, 1114

Theoretical magnetar model

Twist of the external magnetic field

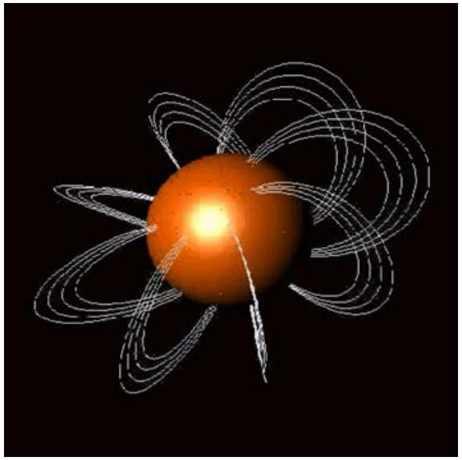

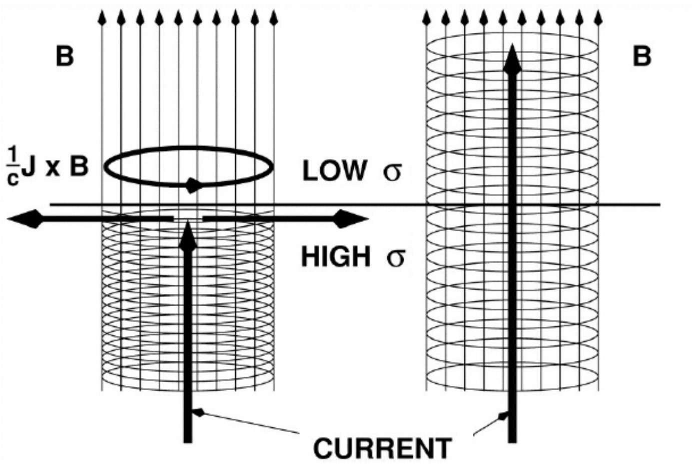

Thomspson, Lyutikov & Kulkarni, 2002 ApJ, 574, 332

- Twist angle:

$$\Delta\phi_{\mathrm{N-S}} = 2 \lim_{\theta\to 0} \int_{\theta}^{\pi/2} \frac{B_{\varphi}}{\sin\theta B_{\theta}} \, \mathrm{d}\,\theta$$

- Giant flares and short bursts are related to the plastic deformation of the crust (or to magnetic reconnection)

- Occurrence of RCS

Photon polarization

- In the presence of strong magnetic fields photons are polarized in two normal modes

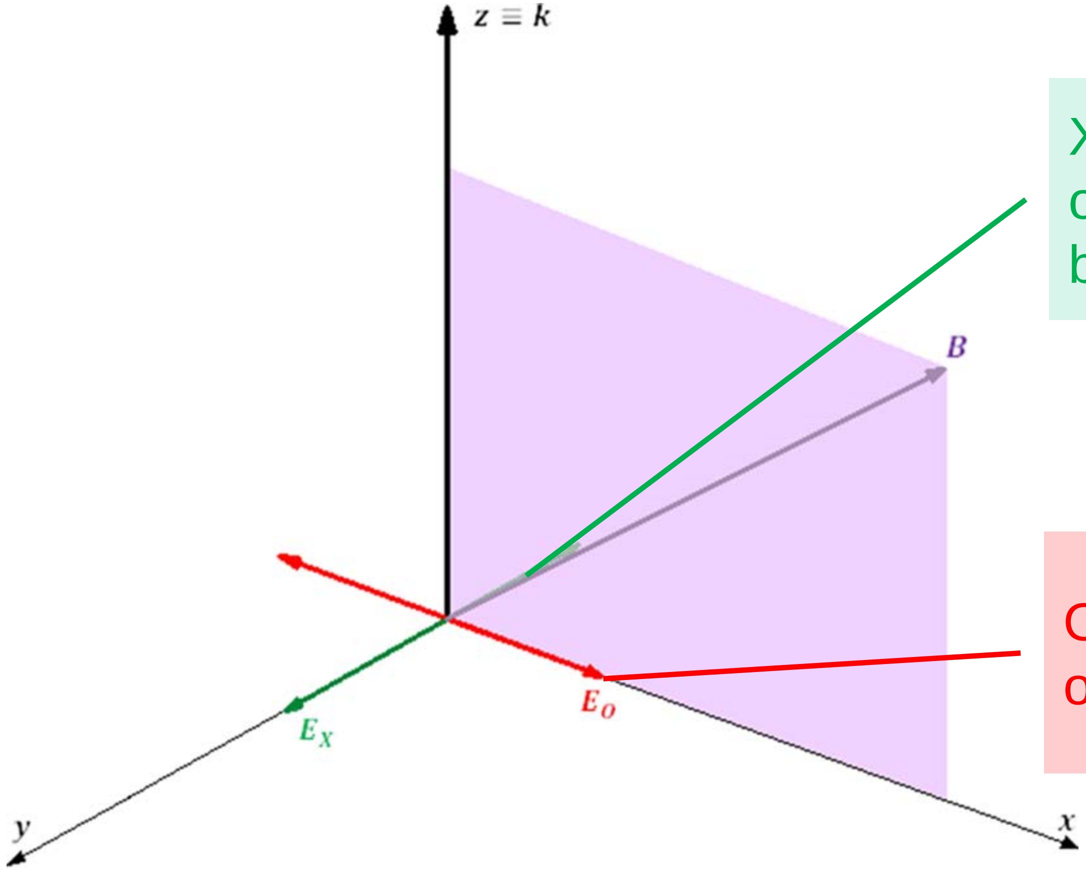

X-mode (photon electric field oscillates perpendicular to both $\boldsymbol{k}$ and $\boldsymbol{B}$)

O-mode (photon electric field oscillates in the $\boldsymbol{kB}$ plane)

Photon polarization

- In the presence of strong magnetic fields photons are polarized in two normal modes

- A convenient way to describe polarized radiation is through the Stokes parameters (that are additive)

$$\boldsymbol{E} = \boldsymbol{A}(z)e^{i(k_0 z - \omega t)}$$

$$\boldsymbol{A} = \left(A_x\, , A_y\right) = \left(a_x e^{-i\varphi_x}, a_y e^{-i\varphi_y}\right)$$

$$\mathcal{I} = A_x A_x^* + A_y A_y^* = a_x^2 + a_y^2$$

$$\mathcal{Q} = A_x A_x^* - A_y A_y^* = a_x^2 - a_y^2$$

$$\mathcal{U} = A_x A_y^* + A_y A_x^* = 2a_x a_y \cos(\varphi_x - \varphi_y)$$

$$\mathcal{V} = i\left(A_x A_y^* - A_y A_x^*\right) = 2a_x a_y \sin(\varphi_x - \varphi_y)$$

Theoretical model

Trapped fireball model

- Alfvén pulses injected by crustal displacements dissipate into a magnetically confined electron-positron plasma

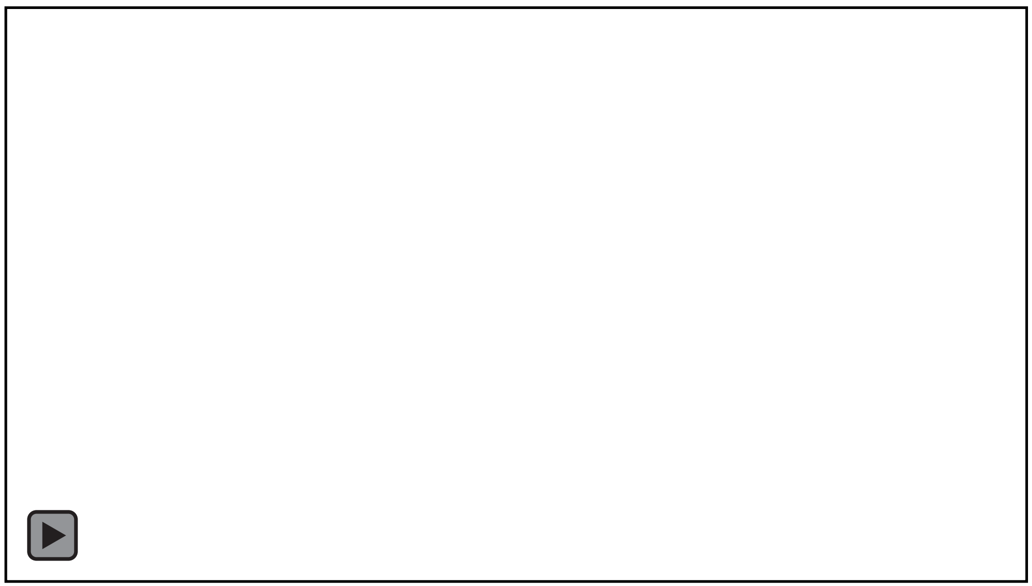

Trapped fireball model

- Alfvén pulses injected by crustal displacements dissipate into a magnetically confined electron-positron plasma

- We assumed the fireball plasma as a pure-scattering medium, restricting our calculations to the Thomson limit

$$\left[\frac{\mathrm{d}^2\sigma}{\mathrm{d}\varepsilon'\mathrm{d}\Omega'}\right]_{\mathrm{OO}} = \frac{3}{8\pi}\sigma_{\mathrm{T}}(1-\mu_{\mathrm{Bk}}^2)(1-{\mu'}_{\mathrm{Bk}}^2)\delta(\varepsilon'-\varepsilon)$$

$$\left[\frac{\mathrm{d}^2\sigma}{\mathrm{d}\varepsilon'\mathrm{d}\Omega'}\right]_{\mathrm{OX}} = \frac{3}{8\pi}\sigma_{\mathrm{T}}\left(\frac{\varepsilon}{\varepsilon_{\mathrm{B}}}\right)^2 \mu_{\mathrm{Bk}}^2\cos^2(\phi_{Bk}-\phi'_{\mathrm{Bk}})\,\delta(\varepsilon'-\varepsilon)$$

$$\left[\frac{\mathrm{d}^2\sigma}{\mathrm{d}\varepsilon'\mathrm{d}\Omega'}\right]_{\mathrm{XO}} = \frac{3}{8\pi}\sigma_{\mathrm{T}}\left(\frac{\varepsilon}{\varepsilon_{\mathrm{B}}}\right)^2 {\mu'}_{\mathrm{Bk}}^2\cos^2(\phi_{Bk}-\phi'_{\mathrm{Bk}})\,\delta(\varepsilon'-\varepsilon)$$

$$\left[\frac{\mathrm{d}^2\sigma}{\mathrm{d}\varepsilon'\mathrm{d}\Omega'}\right]_{\mathrm{XX}} = \frac{3}{8\pi}\sigma_{\mathrm{T}}\left(\frac{\varepsilon}{\varepsilon_{\mathrm{B}}}\right)^2 \sin^2(\phi_{Bk}-\phi'_{\mathrm{Bk}})\,\delta(\varepsilon'-\varepsilon)$$

$$\varepsilon_{\mathrm{B}} = m_{\mathrm{e}}c^2\frac{B}{B_{\mathrm{QED}}}$$

We assumed
$\varepsilon \ll \varepsilon_{\mathrm{B}}$

Second order processes

- Thermal bremsstrahlung
  - $e^- - e^-$ ($e^+ - e^+$) bremsstrahlung strongly suppressed for particle energies < 300 keV ($\sim 0.01\,\sigma_{\rm T}$, Haug, 1975)
  - $e^- - e^+$ bremsstrahlung (slightly enhanced with respect to $e^- - p^+$) becomes negligible above $\varepsilon = 1$ keV and $kT = 10$ keV ($< 0.5\,\sigma_{\rm T}$, Svenson, 1982)

Second order processes

- Thermal bremsstrahlung
- Photon splitting
  - Assuming weak dispersive effects (Stoneham, 1979) the only allowed channel is that of X → OO, for which, in the non-relativistic regime ($\varepsilon \ll m_\mathrm{e}c^2$) and for $B \lesssim B_\mathrm{QED}$

$$\sigma_\mathrm{sp}(\mathrm{X} \to \mathrm{OO}) \propto \left(\frac{B}{B_\mathrm{QED}} \sin\theta_\mathrm{Bk}\right)^6 \left(\frac{\varepsilon}{m_\mathrm{e}c^2}\right)^5 \ll \sigma_\mathrm{T}$$

  - In the strong field limit ($B > B_\mathrm{QED}$) the splitting amplitude decreases exponentially (as $\exp(-B/B_\mathrm{QED})$)

Second order processes

- Thermal bremsstrahlung
- Photon splitting
- Double Compton scattering
  - At energies $\varepsilon \ll kT$ and far from the cyclotron resonance photons are injected in the fireball at a rate (Lightman, 1981)

$$Q \approx \frac{4\alpha_{\mathrm{F}}}{3\pi} \frac{\sigma_{\mathrm{T}}}{m_{\mathrm{e}}^2 c^4} \frac{\exp(\varepsilon/kT) - 1}{\varepsilon^3} [f_{\mathrm{Pl}}(\varepsilon, T) - f(\varepsilon)] I$$

  - At higher energies scattering establishes a Bose-Einstein distribution $f_{BE}(\varepsilon, T)$, but with small chemical potential (see Lyubarsky, 2002)

$$\ln \frac{\mu + \varepsilon_0}{\varepsilon_0} \ll 0.5 \left(\frac{10 B_{\mathrm{QED}}}{B} \right)^2$$

Radiative transfer

Radiative transfer

- We solved the radiative transfer equation in the geometrically thin surface layer of the fireball (see Yang & Zhang, 2015), divided into a number of patches

Radiative transfer

- We solved the radiative transfer equation in the geometrically thin surface layer of the fireball (see Yang & Zhang, 2015), divided into a number of patches

- Assuming the patch dimension small enough the problem can be solved in the plane-parallel approximation

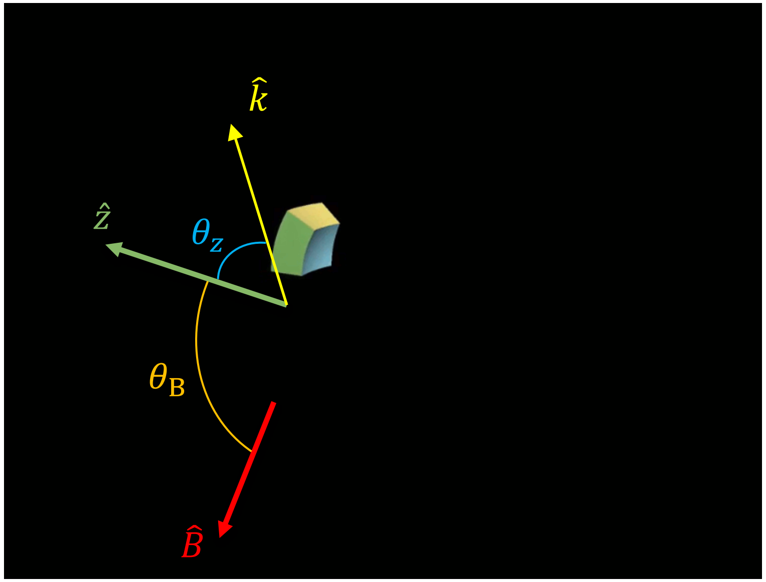

$$\mu_z = \mu_{\mathrm{Bk}}\mu_{\mathrm{B}} - \sqrt{\left(1-\mu_{\mathrm{Bk}}^2\right)\left(1-\mu_{\mathrm{B}}^2\right)}\cos\phi_{\mathrm{Bk}}$$

Radiative transfer equation (RTE)

- Under these assumptions the RTE for the photons polarized in the two modes assumes a simple form

$$\mu_z \frac{\mathrm{d}n_\mathrm{O}}{\mathrm{d}\tau} = -\left[1 - \mu_\mathrm{Bk}^2 + \frac{3\mu_\mathrm{Bk}^2}{4}\left(\frac{\varepsilon}{\varepsilon_\mathrm{B}}\right)^2\right] n_\mathrm{O}(\alpha)$$

$$+\frac{3}{8\pi}\int_{4\pi}\left[(1-\mu_\mathrm{Bk}^2)(1-{\mu'}_\mathrm{Bk}^2)n_\mathrm{O}(\alpha') + \left(\frac{\varepsilon}{\varepsilon_\mathrm{B}}\right)^2 \mu_\mathrm{Bk}^2 \cos^2(\phi_\mathrm{Bk}-\phi'_\mathrm{Bk})\, n_\mathrm{X}(\alpha')\right] \mathrm{d}\Omega'$$

$$\boxed{\mathrm{d}\tau = n_\mathrm{e}\sigma_\mathrm{T}\mathrm{d}s}$$

$$\mu_z \frac{\mathrm{d}n_\mathrm{X}}{\mathrm{d}\tau} = -\left(\frac{\varepsilon}{\varepsilon_\mathrm{B}}\right)^2 n_\mathrm{X}(\alpha) + \frac{3}{8\pi}\left(\frac{\varepsilon}{\varepsilon_\mathrm{B}}\right)^2 \int_{4\pi} [\sin^2(\phi_\mathrm{Bk}-\phi'_\mathrm{Bk})\, n_\mathrm{X}(\alpha')$$
$$+{\mu'}_\mathrm{Bk}^2 \cos^2(\phi_\mathrm{Bk}-\phi'_\mathrm{Bk})\, n_\mathrm{O}(\alpha)]\, \mathrm{d}\Omega'$$

Radiative transfer equation (RTE)

- Under these assumptions the RTE for the photons polarized in the two modes assumes a simple form

- Owing to the suppression factor of the X-mode photon cross sections, the propagation in the fireball medium is quite different according to the polarization mode

$$\tau_{\mathrm{O}} \sim n_{\mathrm{e}}\sigma_{\mathrm{O}}H \approx \tau \qquad \tau_{\mathrm{X}} \sim n_{\mathrm{e}}\sigma_{X}H \approx \left(\frac{\varepsilon}{\varepsilon_{\mathrm{B}}}\right)^2 \tau$$

$$\boxed{\sigma_i = \sigma_{i\mathrm{O}} + \sigma_{i\mathrm{X}}}$$

Ra

- d
- s

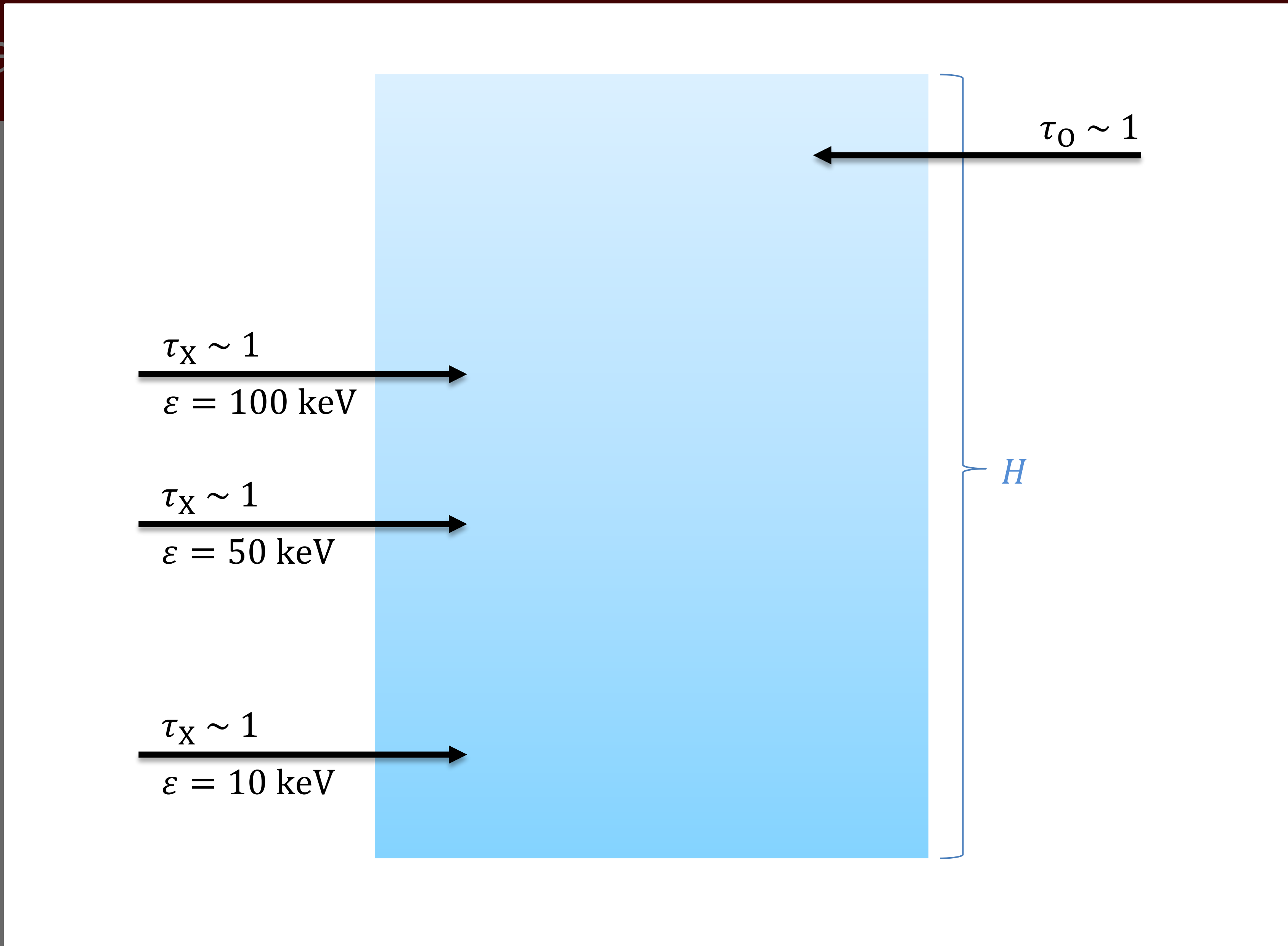
$\tau_O \sim 1$
$\tau_X \sim 1$
$\varepsilon = 100$ keV
$\tau_X \sim 1$
$\varepsilon = 50$ keV
$\tau_X \sim 1$
$\varepsilon = 10$ keV
H

Radiative transfer equation (RTE)

- Under these assumptions the RTE for the photons polarized in the two modes assumes a simple form
- Owing to the suppression factor of the X-mode photon cross sections, the propagation in the fireball medium is quite different according to the polarizati[...]
- Hence we solved the photon trans[...] Rosseland mean optical depth τ_{R} [...]

Temperature distribution
(see Lyubarsky, 2002)

$$T = T_{\mathrm{b}}\sqrt{1+\frac{3}{4}\tau_{\mathrm{R}}}$$

$$\langle\sigma_{\mathrm{X}}\rangle_{\mathrm{R}} = \frac{4\pi^2}{5}\sigma_T\left(\frac{kTB_{\mathrm{QED}}}{m_{\mathrm{e}}c^2B}\right)^2$$

Radiative transfer equation (RTE)

- Under these assumptions the RTE for the photons polarized in the two modes assumes a simple form

- Owing to the suppression factor of the X-mode photon cross sections, the propagation in the fireball medium is quite different according to the polarization mode

- Hence we solved the photon transport in terms of the Rosseland mean optical depth τ_R for the X-mode photons

$$\tau_\mathrm{R} = \frac{4\pi^2}{5}\left(\frac{kT_\mathrm{b}B_\mathrm{QED}}{m_\mathrm{e}c^2B}\right)^2 \sigma_T \int n_\mathrm{e}\mathrm{d}s = R(B)\tau$$

$$\tau_\mathrm{O} = \frac{1}{R(B)}\tau_\mathrm{R} \qquad \tau_\mathrm{X} = \frac{5}{4\pi^2}\left(\frac{\varepsilon}{kT_\mathrm{b}}\right)^2 \tau_\mathrm{R}$$

Numerical implementation and results

Assumptions

- Optical depth in the fireball atmosphere: $\tau_R = 1000$ (at the base) – 0 (at the top)

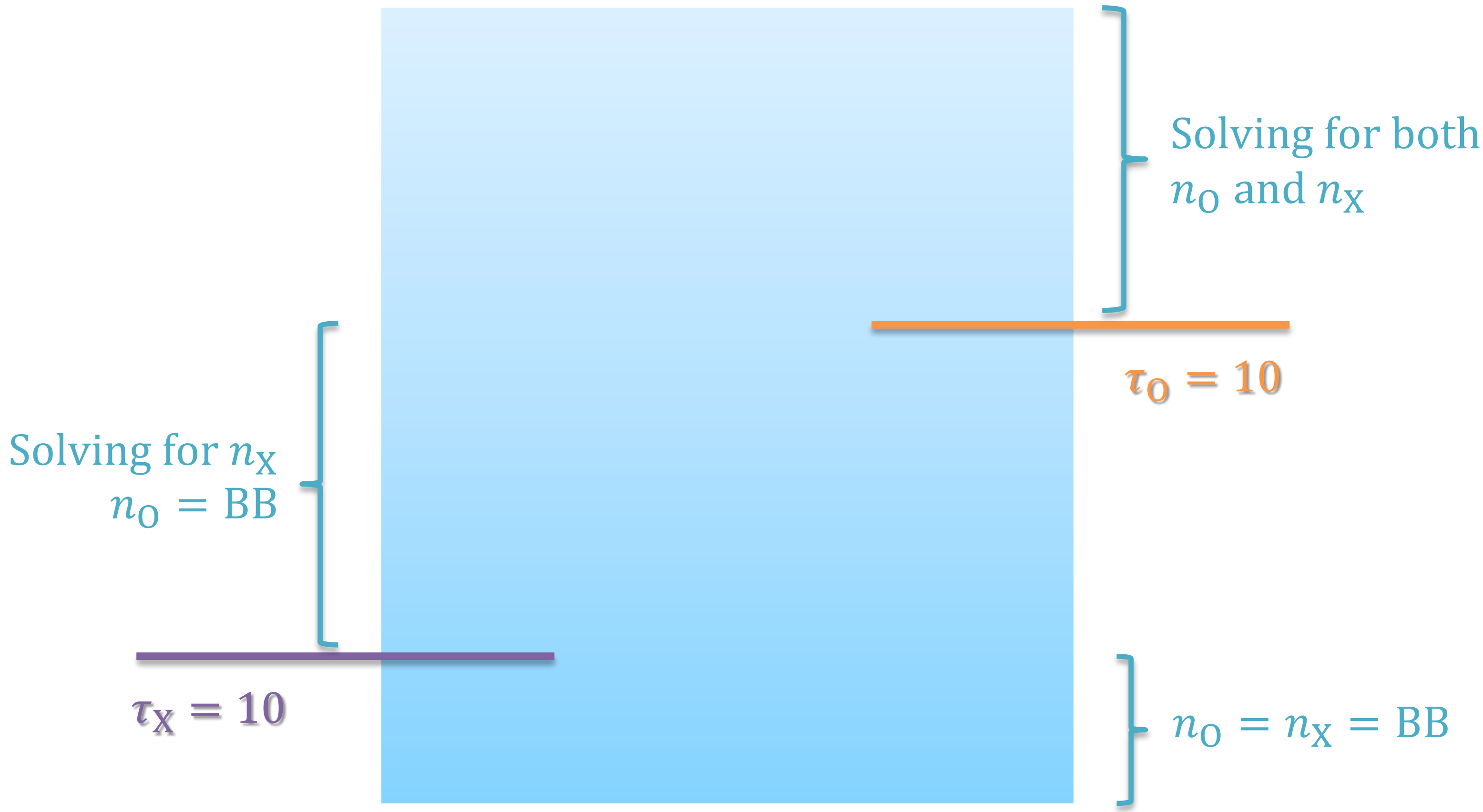

Assumptions

- Optical depth in the fireball atmosphere:
  $\tau_R = 1000$ (at the base) – 0 (at the top)
- Photon energy $\varepsilon = 1 - 100\ \mathrm{keV}$
- Temperature distribution $T = T_{\mathrm{b}}\sqrt{1 + 0.75\tau_{\mathrm{R}}}$ ($T_{\mathrm{b}} = 10\ \mathrm{keV}$)
- Dipolar B-field with $B_{\mathrm{p}} = 2 \times 10^{14}\ \mathrm{G}$
- $R_{\max} = 2R_{\mathrm{NS}}$ ($R_{\mathrm{NS}} = 10\ \mathrm{km}$)

Integration of the RTE

- Λ-iteration method (Runge-Kutta 4th order integration routine)

- Output quantities

$$n_{\mathrm{O}}(\tau_{\mathrm{R}}, \varepsilon, \mu_{\mathrm{Bk}}, \phi_{\mathrm{Bk}}) \qquad n_{\mathrm{X}}(\tau_{\mathrm{R}}, \varepsilon, \mu_{\mathrm{Bk}}, \phi_{\mathrm{Bk}})$$

or

$$n_{\mathrm{O}}(\tau_{\mathrm{R}}, \varepsilon, \mu_{z}, \phi_{z}) \qquad n_{\mathrm{X}}(\tau_{\mathrm{R}}, \varepsilon, \mu_{z}, \phi_{z})$$

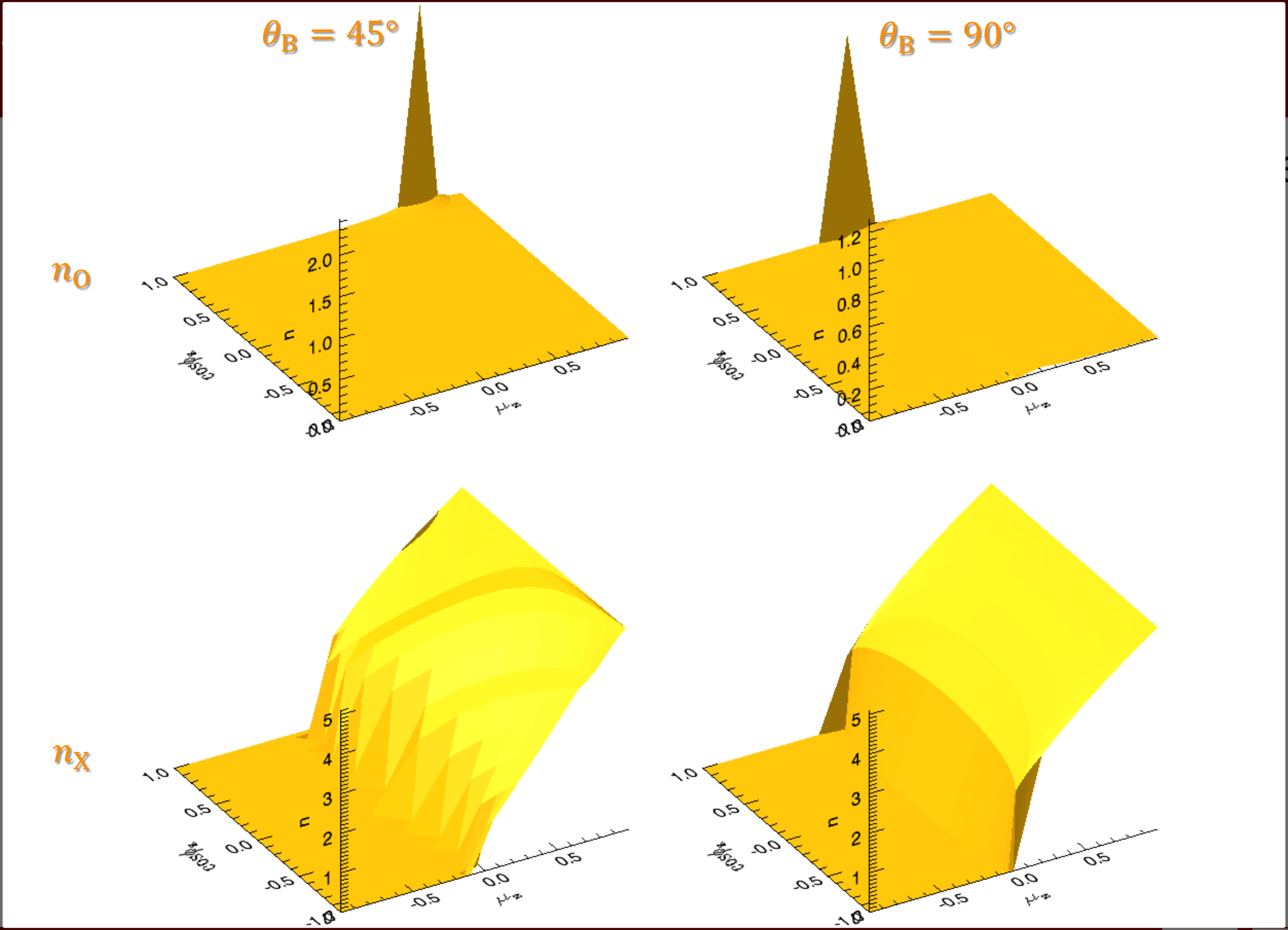
$\theta_B = 45°$
$\theta_B = 90°$
n_O
n_X
n
μ_z
cos φ

In

- e)
-

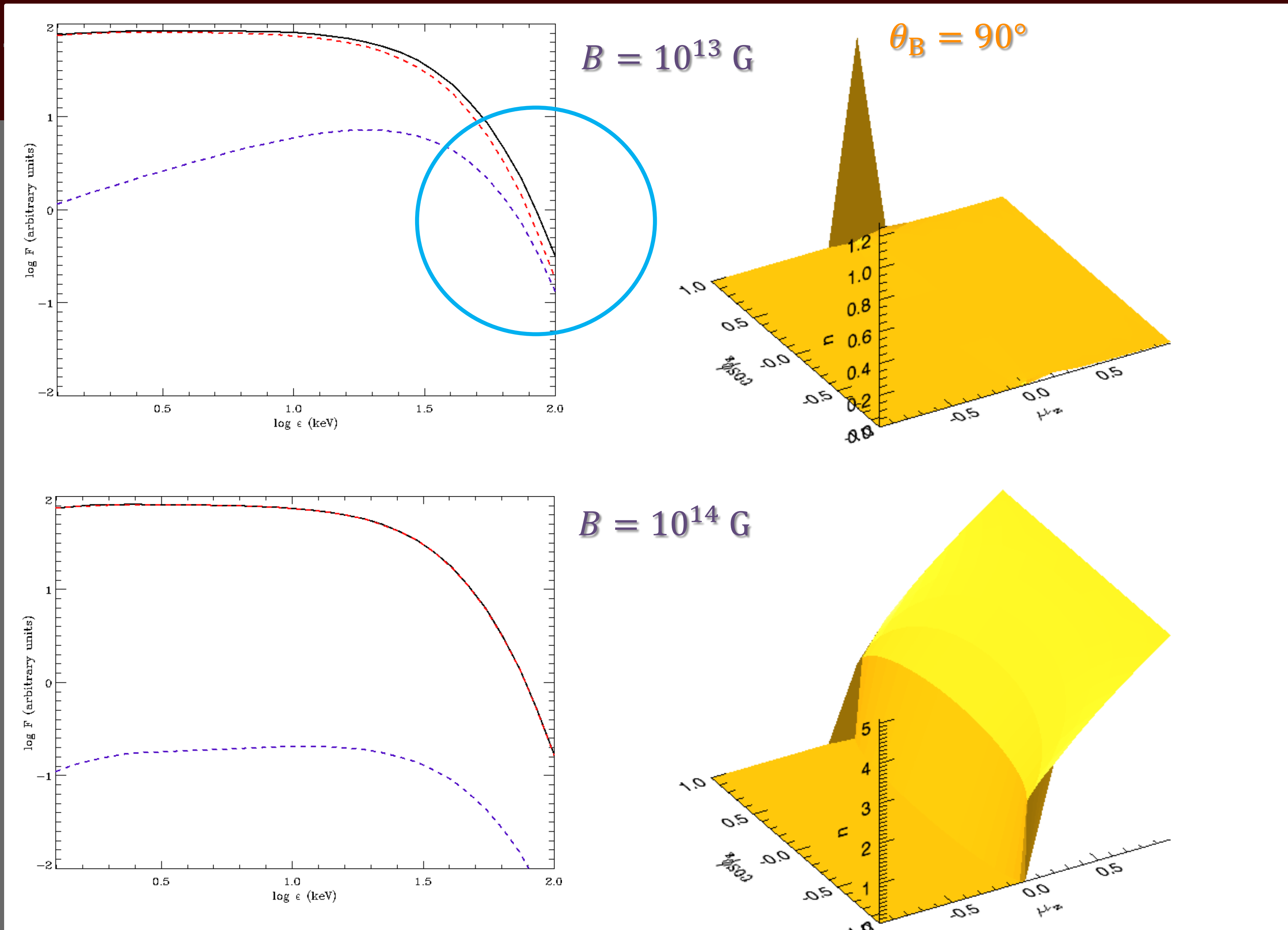

$B = 10^{13}$ G
$\theta_B = 90°$
log F (arbitrary units)
log ε (keV)
$B = 10^{14}$ G
n
cos θ
μ_z

Ray-tracing code

- The contributions from all the patches in view are summed together in a ray tracing code
  - χ angle between ℓ and $\boldsymbol{\Omega}$
  - ξ angle between $\boldsymbol{b}_{\rm dip}$ and $\boldsymbol{\Omega}$
  - ψ angle between $\boldsymbol{u}$ and $\boldsymbol{X}$

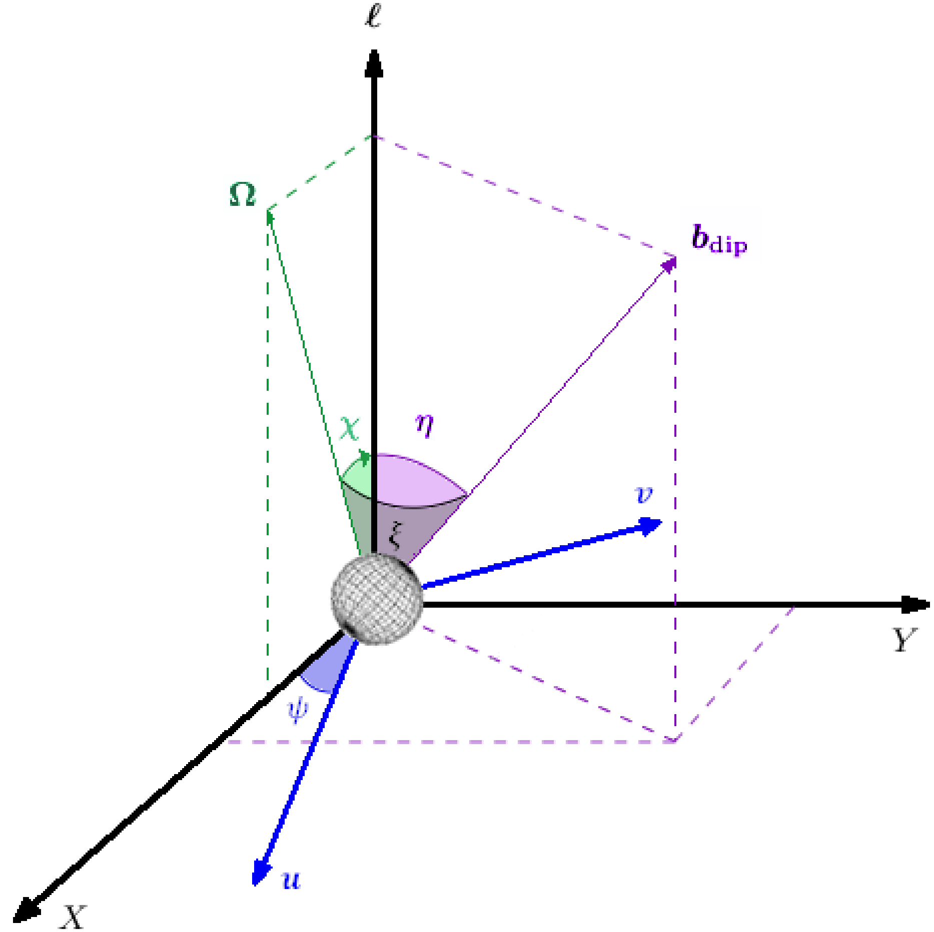

Ray-tracing code

- The contributions from all the patches in view are summed together in a ray tracing code

- Fireball visibility

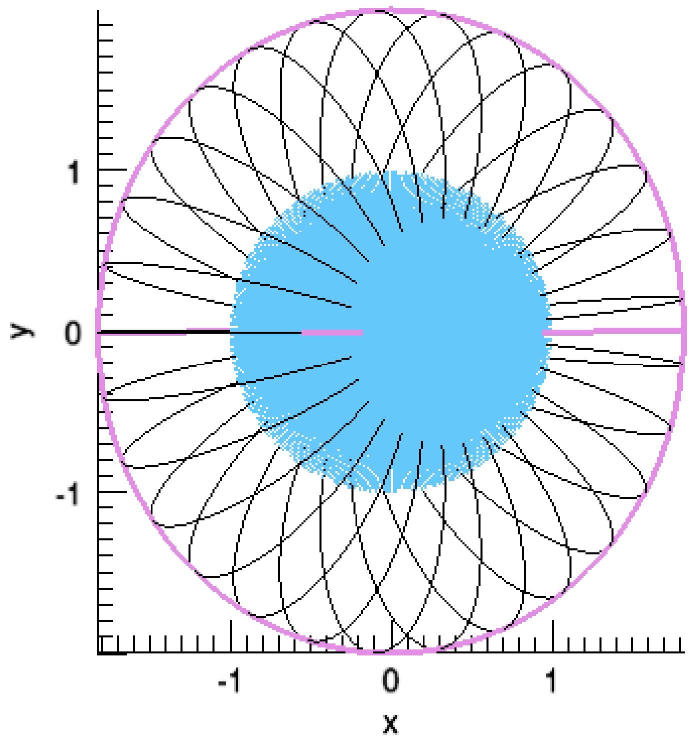

Terminator equation:
$\hat{z} \cdot \hat{\ell} = 0$

Ray-tracing code

- The contributions from all the patches in view are summed together in a ray tracing code
- Fireball visibility
- Different emission geometries

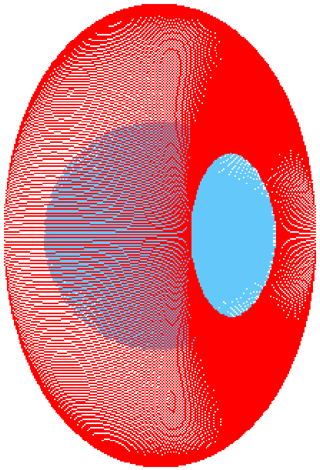

Full torus (model a)

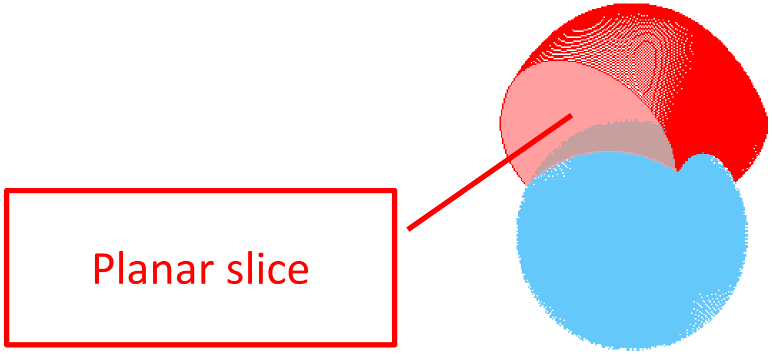

Torus cut (model b)

Ray-tracing code

- The contributions from all the patches in view are summed together in a ray tracing code
- Fireball visibility
- Different emission geometries
- QED and geometrical effects on the polarization observables

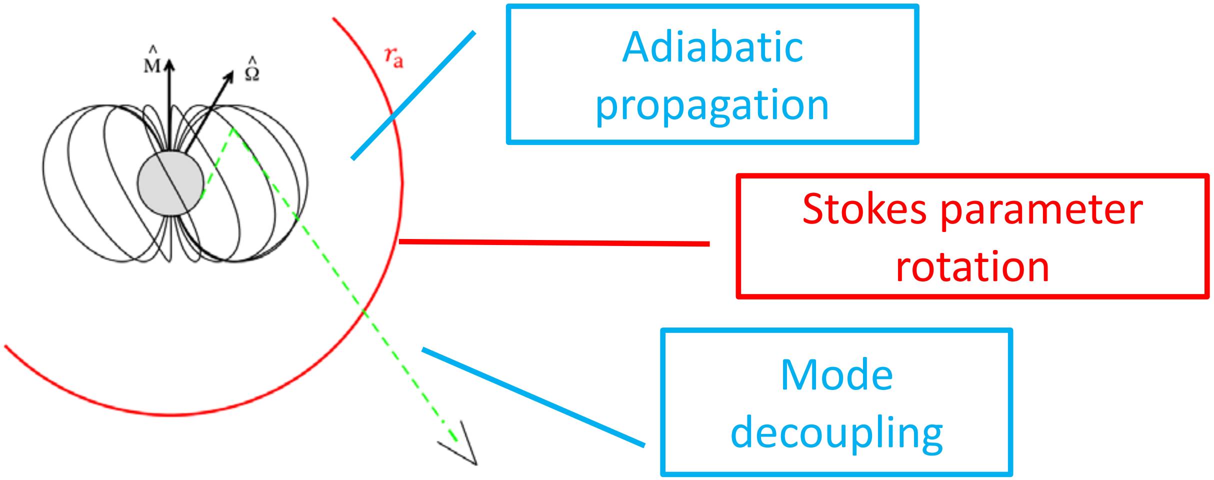

Ray-tracing code

- The contributions from all the patches in view are summed together in a ray tracing code
- Fireball visibility
- Different emission geometries
- QED and geometrical effects on the polarization observables
- Plasma contributions to the dielectric tensor are assumed to be negligible wrt the vacuum terms (vacuum resonance effects are relevant at $\varepsilon \lesssim 1\ \mathrm{keV}$ only, Lyubarsky, 2002)

Spectral analysis

- Phase-averaged spectrum

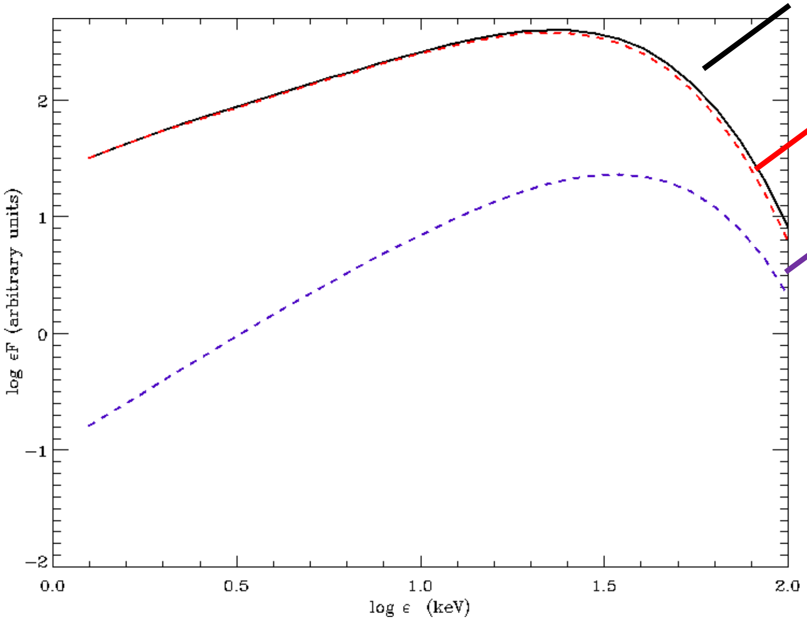

- The total spectrum is nearly superimposed to the X-mode component
- O-mode photon flux strongly suppressed
- High intrinsic polarization degree

Spectral analysis

- Phase-averaged spectrum
- Spectral fit

$$f(\varepsilon) = A_1\varepsilon^3\left(\frac{1}{\exp(\varepsilon/kT_1)-1} + \frac{A_2/A_1}{\exp(\varepsilon/kT_2)-1}\right)$$

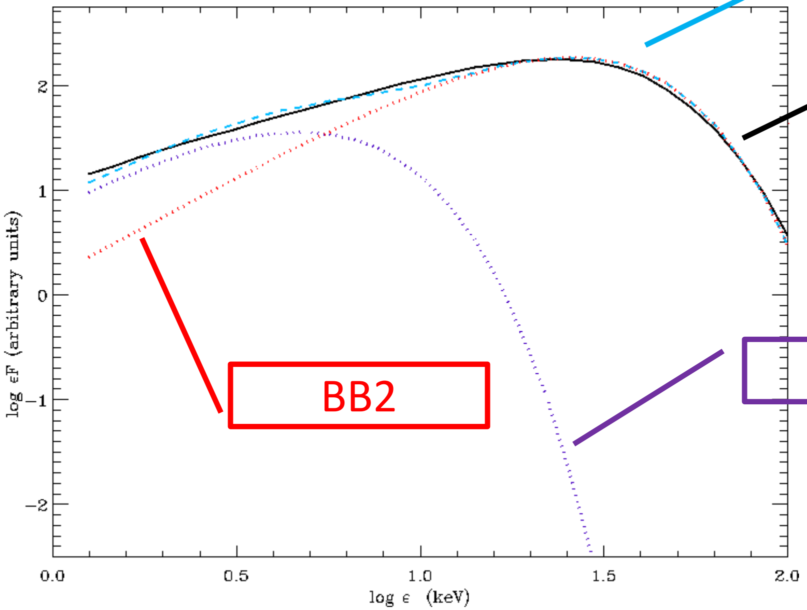

	χ	ξ	T_1 (keV)	T_2 (keV)	R_2/R_1
Model a	60°	30°	1.67	9.11	0.177
Model b	60°	30°	1.67	9.12	0.177
Model a	90°	0°	1.67	9.18	0.178
Model b	90°	0°	1.67	9.14	0.177

Observations of SGR 1900+14 (Israel et al., 2008)

$$T_\mathrm{s} = 4.8 \pm 0.3\ \mathrm{keV} \quad T_\mathrm{h} = 9.0 \pm 0.3\ \mathrm{keV}$$

$$R_\mathrm{h}/R_\mathrm{s} = 0.19 \pm 0.03$$

Spectral analysis

- Phase-averaged spectrum
- Spectral fit
- Pulse profile

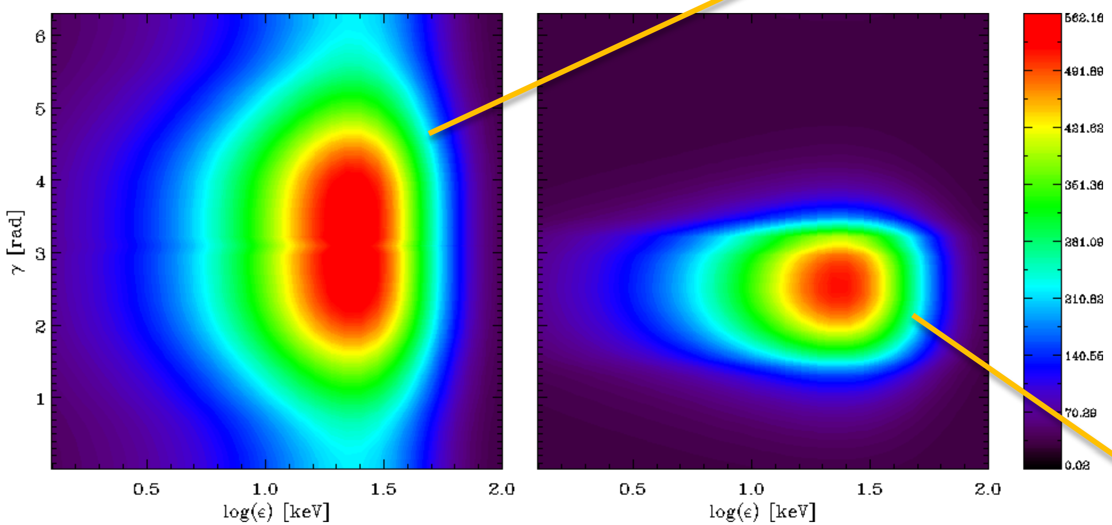

Model a Model b

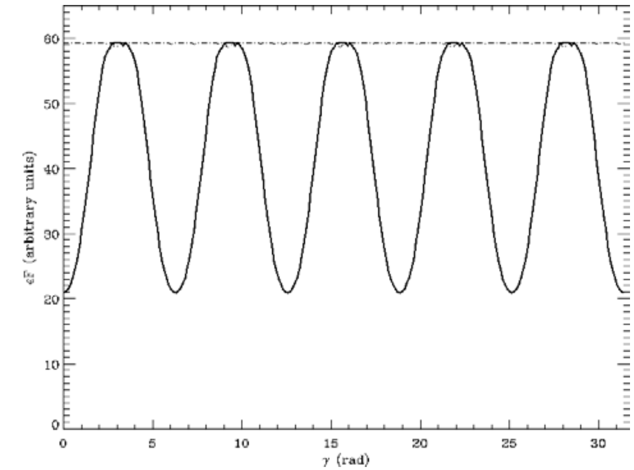

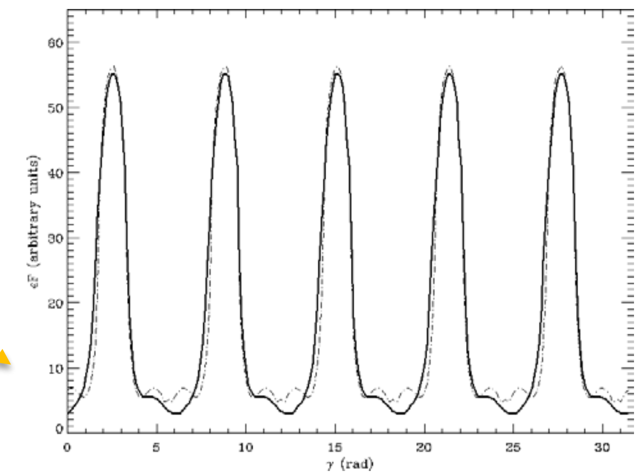

Polarization signal

- Phase-resolved polarization fraction

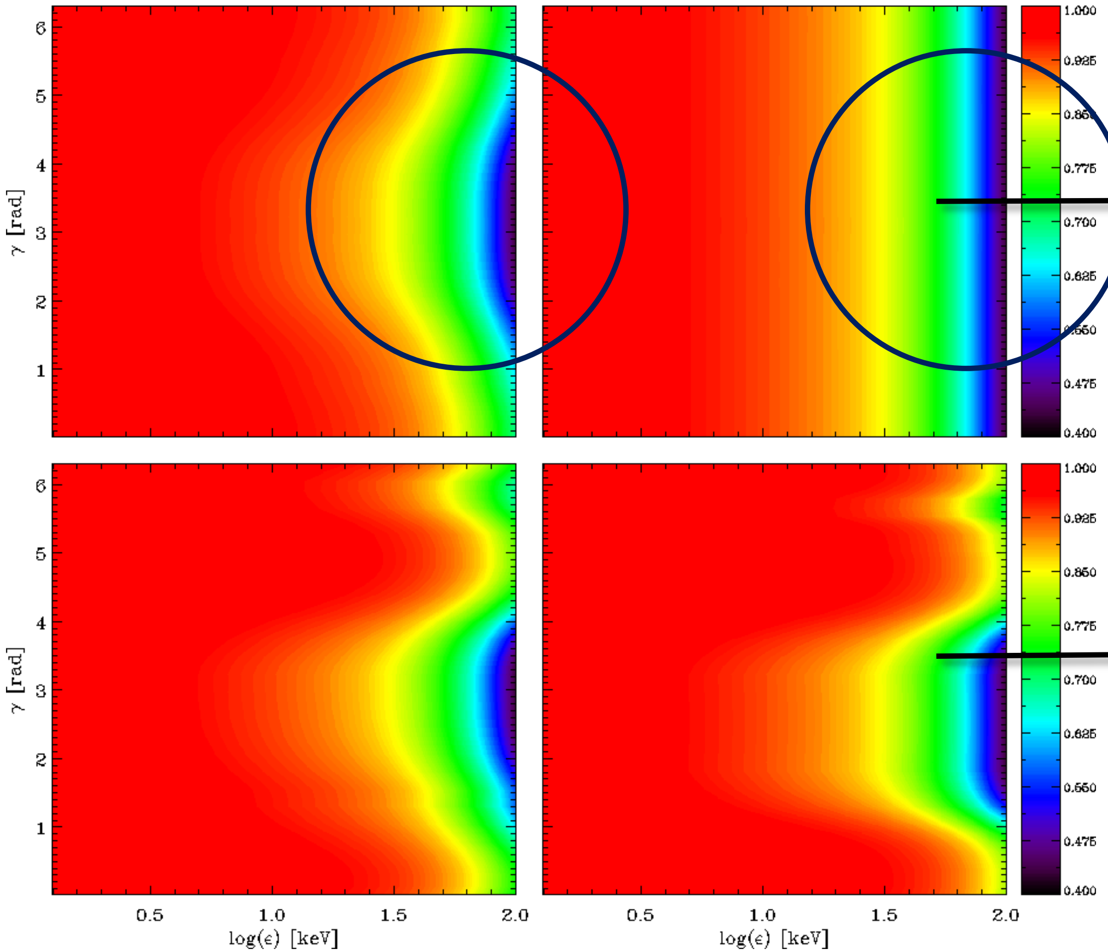

- The PF drops at higher photon energies (where the O-mode contribution becomes more important

Model a

Model b

Polarization signal

- Phase-resolved polarization fraction

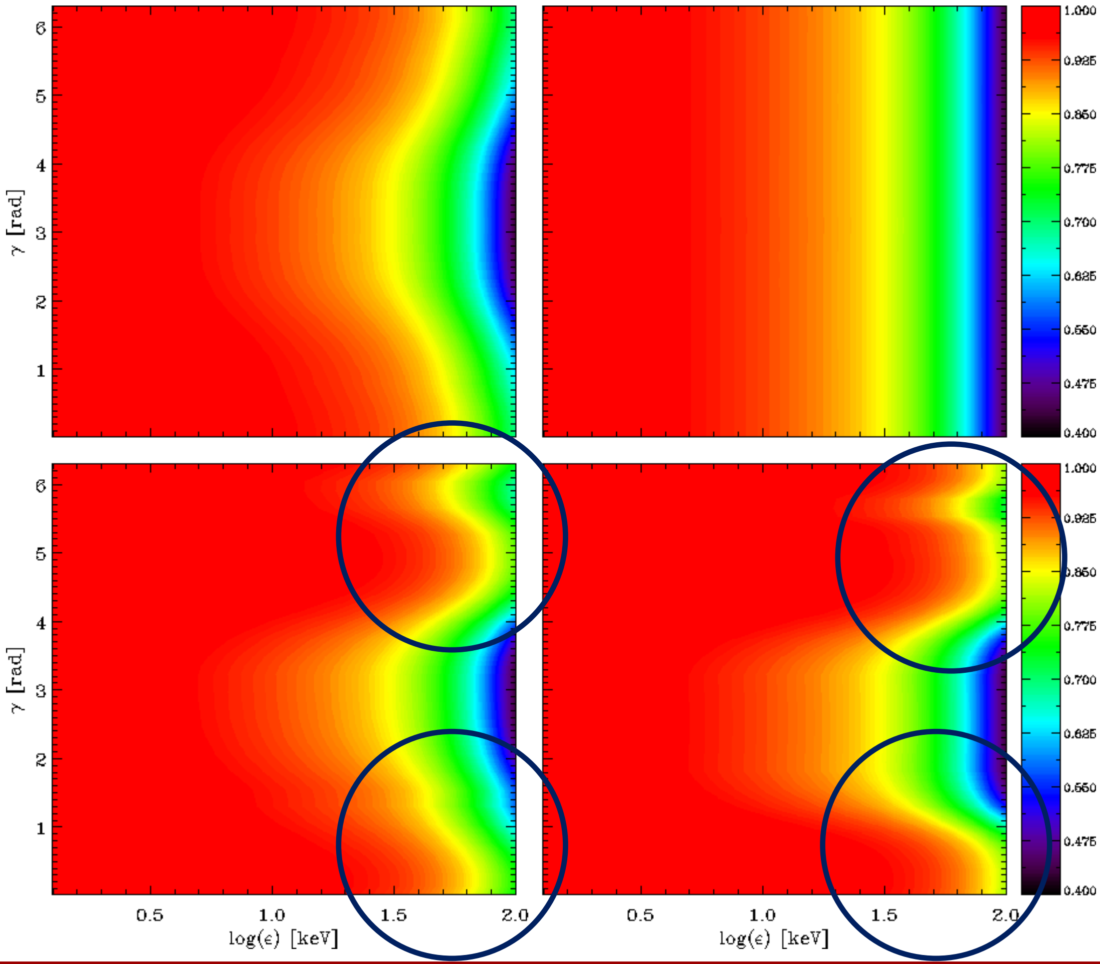

- The PF drops at higher photon energies (where the O-mode contribution becomes more important

- Photons coming from the constant-ϕ cuts are generally more polarized than those coming from the torus

Polarization signal

- Phase-resolved polarization fraction
- Phase-resolved polarization angle

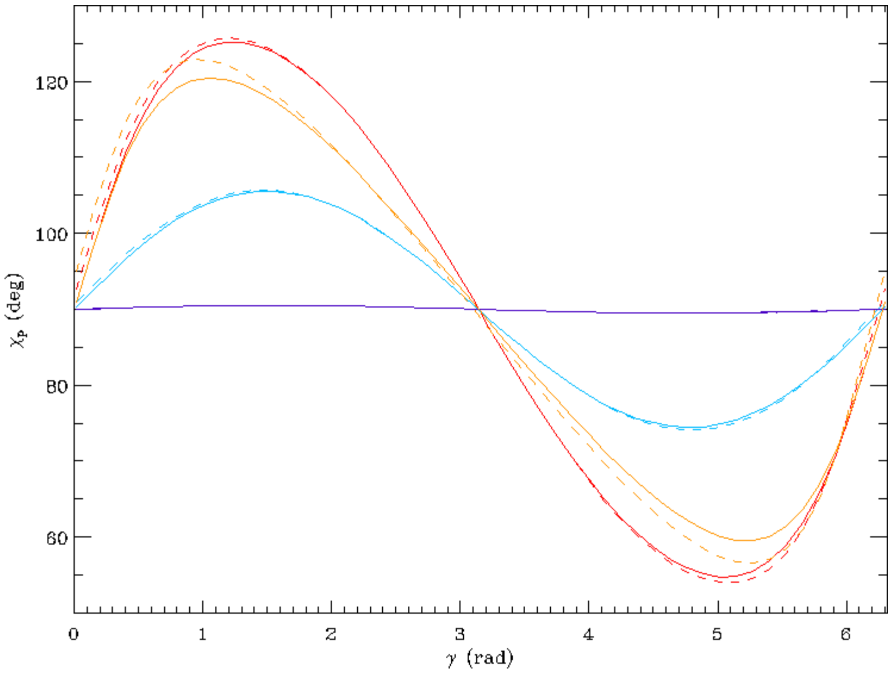

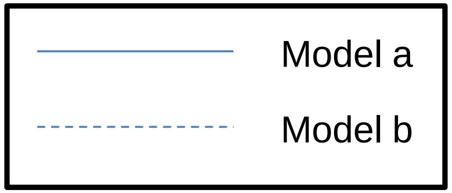

- No substantial differences between model a and model b
- The polarization angle behavior is related to the viewing geometry and the magnetic field topology

Polarization signal

- Phase-resolved polarization fraction
- Phase-resolved polarization angle
- Phase-averaged polarization observables

Model a

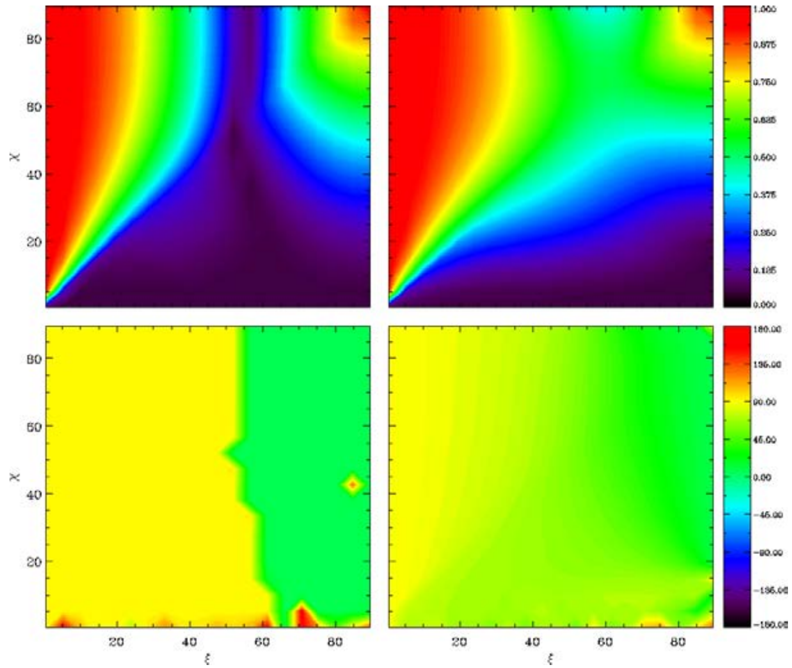

Model b

Conclusions and Future prospects

Conclusions

- Method for modelling the spectral and polarization properties of radiation emitted during magnetar flares from a steady trapped-fireball

- Magnetic (Thomson) scattering is the dominant source of opacity

- Simulated spectra are well fitted by two BB as suggested by observations (but the hypothesis by Israel et al., 2008 of the two different O- and X-mode photospheres is not supported)

- The model can reproduce the pulse profiles observed in intermediate/giant flare decay tails (tuning both viewing and emission geometries)

Conclusions

- Radiation is expected to be highly polarized (in the extraordinary mode)